Excited-State Structural Dynamics of Cytosine from Resonance Raman Spectroscopy

Brant E. Billinghurst and Glen R. Loppnow*

Department of Chemistry, University of Alberta, Edmonton, Alberta T6G 2G2, Canada

Received: October 26, 2005; In Final Form: December 13, 2005

Cytosine, a nucleobase found in both DNA and RNA, is known to form photoproducts upon UV irradiation, damaging the nucleic acids and leading to cancer and other diseases. To determine the molecular mechanism by which these photoproducts occur, we have measured the resonance Raman spectra of cytosine at wavelengths throughout its 267 nm absorption band. Self-consistent analysis of the resulting resonance Raman excitation profiles and absorption spectrum using a time-dependent wave packet formalism yields both the excited-state structural changes and electronic parameters. From this analysis, we have been able to determine that, at most, 31% of the reorganization energy upon excitation is directed along photochemically relevant modes.

Introduction

Deoxyribonucleic acid (DNA), which stores genetic information, and ribonucleic acid (RNA), which mediates translation of the genetic code into proteins, are composed of two purines (adenine and guanine) and three pyrimidines (cytosine, thymine, and uracil);[1] DNA contains adenine, cytosine, guanine, and thymine bases, while RNA contains adenine, cytosine, guanine, and uracil bases. Thus, cytosine (Scheme 1) is the only common pyrimidine base between the two nucleic acids.

Cytosine is of particular interest because of its role in UV-induced DNA damage, which can be linked to skin cancer and other diseases. Scheme 2 shows the possible photoreactions that may occur in cytosine upon UV irradiation. Cytosine dinucleotides (CpC) preferentially form the cyclobutyl photodimer via the [2 + 2] cycloaddition reaction of the C═C on adjacent cytosines with a quantum yield of $\Phi = 0.04$.[2] The [2 + 2] cycloaddition between the C═C bond of one cytosine and the C═O bond of an adjacent cytosine leading to the 6-4 photoadduct is observed in thymine but not in cytosine.[2] The other major photoproduct in CpC is the photohydrate and is formed with $\Phi = 0.006$. However, cytosine can also form photoadducts with thymine; the photodimer ($\Phi = 0.0072$) and the 6-4 photoadduct ($\Phi = 0.00074$) are both observed for cytosine−thymine dinucleotides (dTpdC).[2]

A probe for the initial excited-state structural dynamics is crucial for understanding the subsequent photochemistry of the nucleobases. Femtosecond pump−probe experiments have measured the gas-phase excited-state lifetime for cytosine at 3.2 ps.[3] Time-resolved absorption and fluorescence measurements have shown a shorter lifetime of 0.3−0.76 ps for cytidine and 0.95 ps for cytidine monophosphate.[4−6] However, these rates represent only the electronic relaxation, providing little insight into the molecular structural changes occurring in the photochemically active excited state.

Resonance Raman spectroscopy is a powerful probe of excited-state molecular structure and initial dynamics.[7] By tuning the exciting laser into the absorption band, resonant enhancement of those vibrational modes coupled to the electronic excitation occurs. The resonance Raman vibrational band intensity is directly proportional to the slope of the excited-state potential energy surface along that vibrational coordinate; the greater the change in the molecular structure along the vibrational coordinate, the more intense the resulting resonance Raman band will be. Thus, the intensities of the resonance Raman bands will directly reflect the conformational distortion of the molecule along each of the normal mode coordinates in the excited state.[7]

SCHEME 1

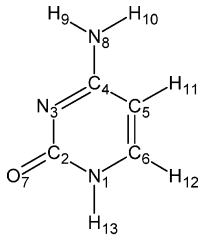

Cytosine

Resonance Raman studies of several deoxyribonucleotides and ribonucleotides have been previously reported.[8−10] However, in none of these studies has a quantitative analysis of the resonance Raman intensities been carried out. Peticolas et al.[11] have attempted to quantify the observed changes in the excited state of cytidine using the Kramers−Kronig transform technique. Reasonably good agreement was found between the observed and calculated absorption spectra. However, the agreement was not as good between the observed and calculated resonance Raman spectra, and the analysis was limited to only the 784, 1243, 1294, and 1529 cm^{-1} vibrational bands.[11]

Previous work investigating the excited-state structural dynamics of thymine and uracil[12] has suggested that their resonance Raman spectra can be used to understand their photochemical differences. That work showed that thymine has much larger molecular distortions along modes that are photochemically relevant, such as the C═C stretching mode (1662 cm^{-1}) and the CH bending mode (1359 cm^{-1}), whereas the majority of the initial dynamics of uracil lay along more dissipative modes.[12] These results suggest that the differences in the photochemistry of thymine and uracil are likely due to greater localization of the vibrations in thymine due to the C_5 methyl group. In this work, we determine the excited-state

* To whom correspondence should be addressed. E-mail: glen.loppnow@ualberta.ca.

10.1021/jp0561571 CCC: $33.50
Published on Web 02/02/2006

SCHEME 2: Photochemistry of Cytosine

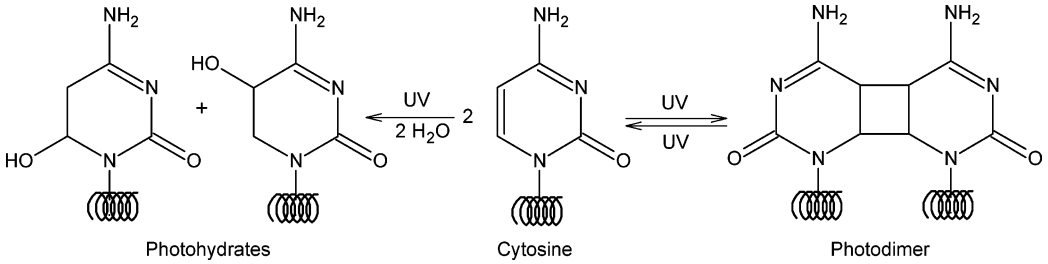

structural dynamics of cytosine (Scheme 1) using the same approach.

Experimental Section

Cytosine (4-amino-2-oxopyrimidine) (99%, Sigma, Oakville, Ontario) and sodium nitrate (99%, EMD Chemicals Inc., Gibbstown, NJ) were used without further purification. All samples were prepared using Nanopure water from a Barnstead water filtration system (Boston, MA).

Laser excitation for the resonance Raman experiments was obtained from a picosecond mode-locked Ti:sapphire laser (Coherent, Santa Clara, CA) pumped with a doubled, continuous wave, solid-state, diode-pumped Nd:YAG laser (Coherent, Santa Clara, CA). To obtain the 244, 257, 266, 275, and 290 nm wavelengths, the output of the Ti:sapphire was doubled using a lithium triborate (LBO) crystal followed by third harmonic generation in a β-barium borate (β-BBO) crystal (Inrad, Northvale, NJ). Typical UV laser powers were 2−20 mW. The resulting laser beam was spherically focused on an open stream of flowing solution in a 135° backscattering geometry. The addition of sodium nitrate as an internal standard had no significant effect on either the absorption or resonance Raman spectra of cytosine. Resonance Raman spectra were obtained using 7 mM cytosine solutions containing 0.2 M sodium nitrate internal standards, at excitation wavelengths of 266, 275, and 290 nm. Sodium nitrate concentrations of 0.01 and 0.04 M were used at excitation wavelengths of 257 and 244 nm, respectively. The resonance Raman scattering was focused into a double-grating spectrometer with a diode array detector. The laser system and spectrometer have been described in detail previously.[13] Measurements of the resonance Raman spectra and determinations of intensities were repeated on three fresh samples of cytosine at each wavelength. Frequency calibration was performed by measuring the Raman scattering of solvents for which the peak positions are known (*n*-pentane, cyclohexane, dimethylformamide, ethanol, acetonitrile, and acetic acid). Frequencies are accurate to ± 2 cm^{-1}. Analyses of the data were performed as previously described.[12] Absorption spectra were acquired before and after each Raman scan using a diode array spectrometer (Hewlett-Packard, Sunnyvale, CA). No significant change in absorbance was observed, suggesting a bulk photoalteration parameter[14−17] below 5%.

The resonance Raman spectra of cytosine in the overtone and combination band region were recorded using the same system as that described for the fundamental region except the 1651 cm^{-1} band was used to scale the spectra and 0.2 M acetonitrile was added to provide a common peak in different spectral windows. The excitation wavelength used for obtaining the overtone region spectra was 257 nm.

The methods used for converting the resonance Raman intensities of cytosine into absolute cross sections and for self-absorption correction have been described previously.[15−17] The experimental nitrate differential cross sections used for this work were 8.74×10^{-11}, 6.35×10^{-11}, 5.67×10^{-11}, 5.31×10^{-11}, and 5.01×10^{-11} Å^2/molecule·sr at 244, 257, 266, 275, and 290 nm, respectively.

Theory

The resonance Raman cross sections were simulated with the time-dependent wave packet formalism[10,18]

$$\sigma_R(E_L) = \frac{8\pi E_S{}^3 E_L e^4 M^4}{9\hbar^6 c^4} \int_0^\infty dE_0 H(E_0) \left| \int_0^\infty dt \langle f|i(t)\rangle \exp\left\{\frac{i(E_L + \epsilon_i)t}{\hbar}\right\} G(t)\right|^2 \quad (1)$$

$$\sigma_A(E_L) = \frac{4\pi E_L e^2 M^2}{6\hbar^2 cn} \int_0^\infty dE_0 H(E_0) \int_{-\infty}^\infty dt \langle i|i(t)\rangle \exp\left\{\frac{i(E_L + \epsilon_i)t}{\hbar}\right\} G(t) \quad (2)$$

where E_L and E_S are the energies of the incident and scattered photons, respectively, M is the transition length, n is the refractive index, $|i\rangle$ and $|f\rangle$ are the initial and final vibrational wave functions in the Raman process, respectively, $H(E_0)$ is a normalized inhomogeneous distribution of zero−zero energies around an average energy ($\bar{E}_0$) expressed as

$$H(E_0) = (2\pi\theta)^{-1/2} \exp\left\{\frac{-(\bar{E}_0 - E_0)^2}{2\theta^2}\right\} \quad (3)$$

with standard deviation θ, $|i(t)\rangle$ is the initial ground-state vibrational wave function propagated on the excited-state potential energy surface expressed as

$$|i(t)\rangle = e^{-iHt/\hbar}|i\rangle \quad (4)$$

and $G(t)$ is the homogeneous line width function. Within the separable harmonic oscillator approximation, the $\langle i|i(t)\rangle$ and $\langle f|i(t)\rangle$ overlaps are dependent only on the difference between the ground- and excited-state equilibrium geometries along each normal mode (Δ). Thus, the resonance Raman intensities directly reflect the dynamics of the excited state.

For molecules interacting with a bath, $G(t)$ represents the dynamics of the chromophore-solvent coupling. The solute-solvent interactions that contribute to the solvent-induced homogeneous broadening are modeled using the Brownian oscillator model developed by Mukamel and co-workers.[19] The general implementation of these equations for absorption and resonance Raman spectroscopy has been described in detail previously.[20,21] In our analysis, we assume that the system remains within the strongly overdamped and high-temperature ($\hbar\Lambda \ll kT$) limits.

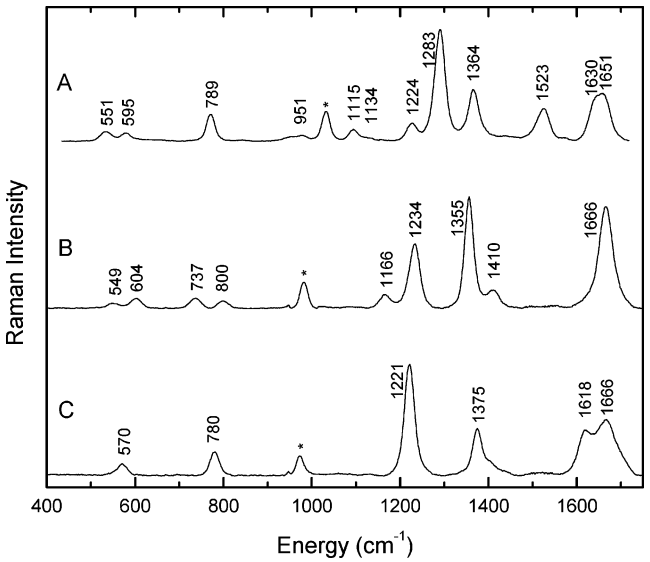

Figure 1. Resonance Raman spectra of 7 mM cytosine (A), 3 mM thymine (B), and 3 mM uracil (C) in water excited at 266 nm. The bands due to the internal standards (0.2 M sodium nitrate for cytosine and 0.4 M sodium sulfate for uracil and thymine) are indicated by asterisks (*).

The initial guesses for the displacements along each normal coordinate (Δ) were based on the assumption that the average relative resonance Raman intensities are proportional to Δ^2, with the intensity of the 1289 cm^{-1} mode arbitrarily set to 1. The relative Δ's were scaled to reproduce the experimentally observed absorption and resonance Raman excitation profile bandwidths. All 12 observed fundamental modes were included in the time-dependent calculations. Overtone vibrations below 3500 cm^{-1} were used to further constrain the simulation. The parameters were then optimized iteratively as described previously[21] until the best possible agreement was obtained for both the calculated and experimental absorption spectra and resonance Raman excitation profiles.

Results

The resonance Raman spectrum of cytosine is shown in Figure 1 and compared with the resonance Raman spectra of thymine and uracil.[12] Twelve bands are observed between 500 and 1700 cm^{-1} for cytosine. These bands have been assigned based on DFT and MP2 calculations done by Gaigeot et al. (Table 1).[22] The most intense band observed for cytosine is the 1283 cm^{-1} band assigned to $\nu(C_2{-}N_3) + \nu(C_4{-}N_8)$. Two overlapping bands are observed at 1630 and 1651 cm^{-1}, attributed to the $\nu(C_5{=}C_6) + \nu(N_3{=}C_4)$ and $\nu(C_2{=}O_7)$ modes, respectively. The bands observed at 789, 1224, 1364, and 1523 cm^{-1} also have fairly high intensities.

Comparing the cytosine spectrum to the spectra of thymine and uracil, several differences are evident. The 1666 cm^{-1} (C=C stretch) band in thymine and the 1618 (C=C stretch) and 1666 (carbonyl stretch) cm^{-1} bands in uracil are relatively more intense compared with the internal standard than the comparable bands for cytosine. There appears to be some similarity between the spectrum of cytosine and that of uracil. Both have two bands around 1650 cm^{-1}, and both have their most intense peak in the 1200−1300 cm^{-1} region. However, cytosine has several more peaks then uracil, and the positions and assignments for some of the peaks are also quite different. Comparing the results here to those of deoxycytidine 5′-monophosphate (dCMP),[8] it is clear that the peak frequencies

TABLE 1: Harmonic Mode Parameters of Cytosine[a]

mode (cm^{-1})	mode assignment[b]	$\lvert\Delta\rvert$[c]	E[d]
551	$\tau(C_4{-}N_8)$ (17), be($N_1C_2O_7$) (12)	0.160	7.0
595	$\tau(C_4{-}N_8)$ (17), be($N_3C_4C_5$) (16)	0.120	4.0
789	$\delta(C_2{=}O_7)$ (74), $\delta(C_4{-}N_8)$ (8)	0.240	23
951	**$\delta(C_6{-}H_{12})$ (61), $\tau(C_5{=}C_6)$ (21)**	**0.105**	**5.0**
1115	be($C_4N_8H_9$) (50), $\nu(N_1{-}C_6)$ (9)	0.170	16
1134	**be($C_6{=}C_5H_{11}$) (27), $\nu(N_1{-}C_6)$ (20)**	**0.180**	**18**
1224	**be($N_1C_6H_{12}$) (19), $\nu(N_1{-}C_6)$ (18)**	**0.350**	**75**
1283	$\nu(C_2{-}N_3)$ (38), $\nu(C_4{-}N_8)$ (13)	0.950	580
1364	**$\nu(C_4{-}N_8)$ (18), be($C_5C_6H_{12}$) (17)**	**0.600**	**250**
1523	$\nu(C_4{-}N_8)$ (17), $\nu(N_3{=}C_4)$ (14)	0.410	130
1630	**$\nu(C_5{=}C_6)$ (32), $\nu(N_3{=}C_4)$ (13)**	**0.340**	**94**
1651	$\nu(C_2{=}O_7)$ (76)	0.540	240

[a] The frequencies listed are the experimental frequencies reported here. [b] Abbreviations: ν, stretching; δ, deformation; be, bending; τ, torsion. Assignments are from ref 22. The numbers in parentheses represent the percentage potential energy distribution (PED) of the listed internal coordinate(s) to the normal mode. Only the two major internal coordinates are listed. [c] Displacements (Δ) are in units of dimensionless normal coordinates and were obtained by fitting eqs 1 and 2 with the following parameters: temperature $T = 298$ K, Brownian oscillator line shape $\kappa = \Lambda/D = 0.1$, Gaussian homogeneous line width $\Gamma_G = 185$ cm^{-1}, inhomogeneous line width $\theta = 1150$ cm^{-1}, zero−zero energy $E_0 = 35\,900$ cm^{-1}, and transition length $M = 0.61$ Å. The estimated errors in the parameters used in the calculation are as follows: $E_0 \pm 1\%$, $M \pm 1\%$, $\Gamma \pm 5\%$, $\theta \pm 5\%$, and $\Delta \pm 5\%$. [d] E is the reorganization energy, in wavenumbers, calculated using eq 6.

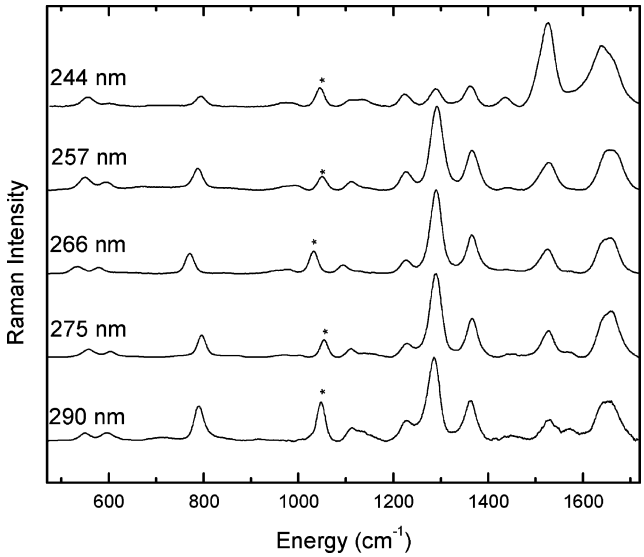

Figure 2. Resonance Raman spectra of cytosine at excitation wavelengths within the 267 nm absorption band. The asterisk (*) in each spectrum indicates the nitrate internal standard peak. Spectra have been scaled to the height of the largest peak in each spectrum and off-set along the ordinate for clarity.

are approximately the same in the UV resonance Raman of the two but that the relative intensities are very different for almost every peak. For example, the 789 cm^{-1} band is far more intense in dCMP than in cytosine.

The spectra of cytosine at different excitation wavelengths within the 267 nm absorption band are compared in Figure 2. Apart from excitation at 244 nm, there are no frequency shifts or relative intensity changes as the Raman excitation wavelength is scanned through the absorption band, indicating that the Raman spectra are enhanced by a single electronic transition. At 244 nm, the resonance Raman spectrum changes significantly. The 1523 cm^{-1} band becomes the most intense band in the spectrum, with increased intensity also observed in the 1630

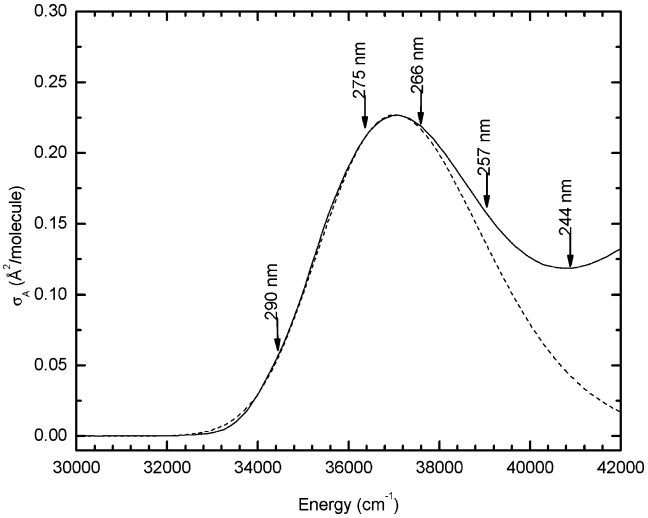

Figure 3. Experimental (solid line) and simulated (dotted line) absorption spectra of cytosine. The simulated absorption spectrum was calculated with eq 2 by using the parameters in Table 1. Discrepancies observed above 38 000 cm^{-1} are due to higher-energy electronic transitions which were not modeled.

cm^{-1} band. These results suggest that enhancement of the vibrations by the ~200 nm absorption band is becoming a factor at this excitation wavelength. However, because the resonance enhancement from the 200 nm absorption band is weak at 244 nm, this electronic transition has little effect on the measured resonance Raman excitation profiles (Figure 4).

The experimental and simulated absorption spectra are shown in Figure 3, while the simulated and experimental resonance Raman profiles are shown in Figure 4. Figures 3 and 4 show good agreement between the experimental and calculated resonance Raman profiles and absorption spectra. Deviations between the experimental and calculated absorption spectra which appear above 38 000 cm^{-1} are attributed to higher-energy electronic transitions which are not modeled here. The different relative Raman intensities of the vibrational bands seen in Figure 1 are directly reflected in the different experimental Raman cross sections (Figure 4) and excited-state geometry displacements (Table 1).

To better constrain the parameter set which accurately describes the absorption spectra and fundamental resonance Raman excitation profiles, the overtones and combination bands between 1700 and 2900 cm^{-1} were also measured at an excitation wavelength of 257 nm. Although some overtones are expected at frequencies greater than 2900 cm^{-1}, these were obscured by the broad O−H stretching vibrations of water. It is well-known that the overtone and combination band intensities are also sensitive to the excited-state geometry displacements (Δ's), and provide an additional constraint on the excited-state parameters. The experimental and calculated cross sections for all of the observed overtone and combination bands of cytosine are given in Table 2. The experimental cross sections of most of the overtone and combination bands are reproduced well using the parameters in Table 1. Of all the measured overtone and combination bands, only the experimental cross sections of the 2566 and 2650 cm^{-1} bands are not reproduced well with the parameters of Table 1. This discrepancy could be attributed to an undulating baseline in the 2400−2800 cm^{-1} region of the experimental resonance Raman spectrum. The good agreement in the other overtones and combinations of the fundamentals that make up these two bands supports this suggestion. These results show that the analysis presented here is an accurate reflection of the excited-state structural dynamics of cytosine.

Discussion

Photochemical Structural Dynamics. To evaluate the excited-state structural dynamics of cytosine, accurate descriptions of the vibrational modes are required. There are several papers that attempt to describe the vibrational modes of cytosine.[22−24] Work by Santamaria et al.[23] used the highest basis set (6-311G) of three treatments at the BP83 level of theory to calculate the vibrational modes of cytosine. However, more recent work by Gaigeot et al.[22] used the higher B3LYP and MP2 levels of theory with a 6-31G* basis set. For this reason, the potential energy distribution from Gaigeot et al.[22] was chosen here for the vibrational assignments. In most cases, the assignments could be made in a fairly straightforward manner by comparing the observed and predicted peak positions. The only exceptions are the peaks at 1630 and 1651 cm^{-1}. These peaks have been assigned here to the $\nu(C_5{=}C_6) + \nu(N_3{=}C_4)$ and $\nu(C_2{=}O_7)$ modes which were calculated to appear at 1708 and 1820 cm^{-1}, respectively. These assignments were based on work by Fodor et al.[8] in which the band observed at 1652 cm^{-1} is assigned to the C═O stretch, due to its shift upon ^{18}O substitution. In that same work, the peak at 1588 cm^{-1} is assigned to the N═C and C═C stretches due to its shift in D_2O.[8] Furthermore, earlier work by Aamouche et al.[24] assigned these vibrations to the C═N + C═C and C═O stretches, respectively, even though the calculations predict them to be higher in energy. That paper used similar methods to those used by Gaigeot et al. and obtained similar results for the potential energy distribution (PED).

Considering the UV-induced photochemical products of cytosine and that the resonance Raman intensity is roughly proportional[10] to Δ^2, one can predict which vibrational modes will have resonance Raman intensity, assuming that the initial excited-state structural dynamics lie along the photochemical reaction coordinate. For the formation of either the photodimer or the photohydrate, there are two significant changes that occur during the photochemical reaction. One is that the $C_5{=}C_6$ double bond becomes a single bond. Therefore, one would expect to see a high resonance Raman intensity for bands involving the C═C stretch. Also, the hybridization of the C_5 and C_6 carbons goes from sp^2 to sp^3. Therefore, modes involving either CH bending, deformation, or wagging on those carbons would be expected to have significant intensity.

Using these vibrational assignments and the predicted intense modes in the resonance Raman spectra of cytosine, five bands may be identified as being photochemically relevant (bold entries, Table 1). The most intense of these are the 1630 ($C_5{=}C_6$ stretch), the 1224 ($N_1C_6H_{12}$ bend), and 1364 ($C_5C_6H_{12}$ bend) cm^{-1} bands. The other two photochemical bands are the 951 and 1134 cm^{-1} bands and involve bends and deformation about C_6 and/or C_5. The latter bands are much weaker then the former three bands. It must be noted here that the designation of modes as photochemically relevant or not is somewhat subjective, due to the incomplete vibrational assignments previously reported.[22] It should also be noted that the modes that are being designated as being photochemically relevant have at least one of the two largest PEDs along a photochemical internal coordinate but that motion is only a portion of the mode. Additionally, some of the other modes may contain a small component along the photochemical reaction coordinate. Nevertheless, these assignments still provide a reasonable comparison of the excited-state structural dynamics among the pyrimidine nucleobases.

The results found in this work can be compared to computations of the formation of cytosine cyclobutane photodimers.[25]

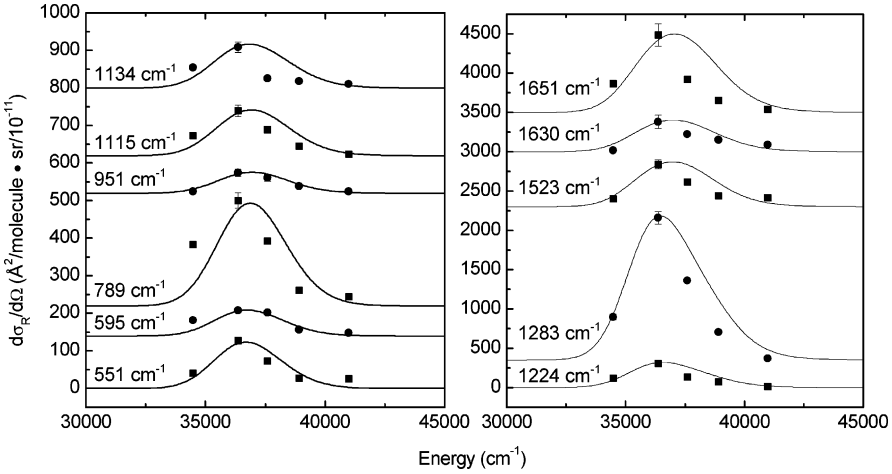

Figure 4. Experimental (points) and calculated (solid lines) resonance Raman excitation profiles of cytosine. The excitation profiles were calculated with eq 1 by using the parameters in Table 1. The excitation profiles have been off-set along the ordinate for greater clarity of presentation. Error bars are on the order of the point size unless otherwise indicated.

TABLE 2: Experimental and Calculated Resonance Raman Overtone and Combination Band Cross Sections for Cytosine[a]

mode (cm^{-1})	assignment	exptl $d\sigma_R/d\Omega$ ($Å^2$/molecule·sr/10^{-11})	calcd $d\sigma_R/d\Omega$ ($Å^2$/molecule·sr/10^{-11})
2074	1283 + 789	65 ± 5	51
2157	1361 + 789	24 ± 5	23
2450	(1224 × 2) + (1283 + 1115) + (1283 + 1134)[b]	91 ± 27	66[b]
2518	1361 + 1150	13 ± 6	12
2566	1283 × 2	118 ± 38	351
2650	1361 + 1283	146 ± 36	280
2737	1361 × 2	98 ± 30	86
2812	1651 + 1224	41 ± 25	41

[a] The excitation wavelength is 257 nm. Cross sections were calculated with eq 1 by using the parameters of Table 1. [b] These modes could not be resolved in the experimental data. The calculated cross section includes all three vibrations.

This computation predicts that the transition-state structure has a $C_5{=}C_6$ bond length increasing by 0.136 Å in one cytosine and by 0.053 Å in the other. From the work done here, the resonance Raman-determined dimensionless displacement (Δ) can be used to calculate the change in bond length (δR) by using the following relation

$$\delta R = (\hbar/\mu\omega)^{1/2}\Delta \qquad (5)$$

where μ is the reduced mass and ω is the average frequency. Treating C=C as an isolated bond and assuming an average frequency of 1600 cm^{-1} for all of the modes that contain the C=C stretch, a δR value of 0.05 Å is found. This is obviously a simplified model, which is necessary due to the limitations of the normal mode description used. However, considering the simplicity of the model, this result still compares favorably with the computational results for one of the cytosines,[25] suggesting that the resonance Raman intensities are reflecting accurate structural distortions in the excited state.

Using these assignments and the relation

$$E = {}^1/_2\Delta^2\tilde{\nu} \qquad (6)$$

the reorganization energy (E) can be calculated from the frequencies ($\tilde{\nu}$ in cm^{-1}) and Δ's given in Table 1. Taking the sum of all of the photochemically relevant modes (shown in bold, Table 1) as a percentage of the total reorganization energy for all of the modes, we see that 31% of the reorganization energy involved in the transition occurs along photochemically relevant modes. This result can be considered an upper limit for the percentage of reorganization energy directed along the photochemically relevant coordinates. Similar analyses of thymine and uracil excited-state structural dynamics show that 66 and 13%, respectively, of their reorganization energy is along photochemically relevant coordinates.[12] This would suggest the amount of reorganization energy directed along the photochemical coordinate in cytosine falls between that of thymine and uracil. If the reorganization energies for the photochemically relevant modes are scaled to reflect the percentage of the said mode which is along a photochemically relevant coordinate, then the percentage of the reorganization energy along the photochemical reaction coordinate is reduced to only 7%.

Considering the relative amounts of reorganization energy along the photochemical coordinates for cytosine, thymine, and uracil and the photoproducts of these molecules, a qualitative model can be developed. Of the three, thymine has the largest percentage of its reorganization energy along the photochemical coordinate (66%),[12] and its photoproducts are primarily the cyclobutyl dimer and the 6-4 photoadduct. Uracil has only 13% of its reorganization energy along the photochemical coordinate,[12] and the primary photoproduct is the photohydrate, with a small amount of the cyclobutyl dimer. Cytosine falls between thymine and uracil, with up to 31% of the reorganization energy along the photochemical coordinate. Like thymine, the primary cytosine photoproduct is the cyclobutyl dimer, but the secondary product is the photohydrate. These results show a clear correlation between the amount of reorganization energy along the photochemical reaction coordinate and the nature of the photoproducts formed, suggesting that the potential energy surfaces for the photochemical reactions of these molecules are similar. These results also suggest that the photochemistry is determined by the initial excited-state structural dynamics in the lowest-lying ($\pi\pi^*$) state.

It is evident from the resonance Raman spectra (see Figure 2) that the 1523 and 1630 cm^{-1} bands are resonant with a second, higher-lying excited electronic state, since the relative intensities of these bands increase relative to the rest of the bands at the 244 nm excitation wavelength. It is likely that these bands are resonant with the 235 or 205 nm band absorption of cytosine, both of which are higher-energy ($\pi\pi^*$) transitions.[26] Both the 1630 and 1523 cm^{-1} modes contain at least some amount of

C═N stretch, suggesting that these higher-lying ($\pi\pi^*$) transitions likely involve large changes in the C═N bond length. Similar observations have been made in the resonance Raman spectra of dCMP.[8] This observation also agrees with the electronic structure calculations done by Hug and Tinoco,[27] which showed that the 267 nm band has its major transition dipole component along the C_5═C_6 bond and that the 235 nm band has its major transition dipole component along the C═N bond with a strong component from the exocyclic nitrogen. Furthermore, calculations by Peticolas et al.[28] showed that excitation at 266 nm caused a change in the C_5═C_6 bond order roughly 3 times the change for the C═N bond and that the opposite was observed for excitation at 213 nm. Note that it has been previously shown that the 235 and 205 nm bands are either similar or one of them does not cause significant enhancement, as the resonance Raman spectra taken in these regions show similar patterns.[8,28]

Broadening. Solvents may contribute significantly to the breadth of the absorption spectrum in the condensed phase through either inhomogeneous or homogeneous mechanisms. These two factors affect the observed absorption spectrum and resonance Raman excitation profiles differently. The inhomogeneous line width is due to ensemble "site" effects, while the homogeneous line width represents contributions from excited-state population decay and pure dephasing. The relative contributions of these two broadening terms cannot be determined using the absorption spectrum alone, as they both broaden the absorption spectrum. However, homogeneous broadening also damps the resonance Raman excitation profile. For cytosine, both the inhomogeneous and homogeneous line widths must be relatively large to reproduce the experimental absorption spectrum and resonance Raman excitation profiles. Although solvent-induced dephasing is normally the dominant homogeneous broadening mechanism in the condensed phase, population decay may also contribute because of the rapid excited-state decay time of cytosine. To accurately model the magnitude of the resonance Raman cross sections and the diffuse absorption spectrum, a Gaussian homogeneous line width of 185 cm^{-1} was required. Nonradiative processes, primarily internal conversion, are known to be the primary population decay mechanism for cytosine because of the low quantum yields for fluorescence ($\sim 10^{-4}$) and photoproduct formation (0.04−0.006).[2] Since the excited-state lifetime of cytosine is 1.1 ps,[29] a Lorentzian homogeneous line width in energy of $\sim$5 cm^{-1} would be obtained. However, the absorption spectrum and resonance Raman excitation profiles of thymine and uracil indicate that the homogeneous line width is primarily Gaussian in shape and much larger in energy. The exponential line shape can be converted to a Gaussian by assuming that the time integrals of both functions are identical. This yields a relation between the Lorentzian and Gaussian line widths of $\Gamma_G = \Gamma_L(\pi/4)^{1/2}$, yielding a Gaussian line width of 4.7 cm^{-1}. Since this Gaussian population decay line width is much too low to account for the breadth of the absorption spectrum and the magnitude of the resonance Raman cross sections, compared to the 185 cm^{-1} value used here, it follows that solvent-induced dephasing is the primary contributor to the homogeneous line width.

The inhomogeneous broadening arises because there can be a number of different solvation structures in solution leading to a distribution of electronic transition energies. Inhomogeneous broadening is considered static on the time scale of the resonance Raman experiment. It has already been noted that the inhomogeneous broadening needed to fit the data for cytosine is quite high (1150 cm^{-1}). This result has been predicted in previous work done by Leszczynski et al.[30,31] using DFT methods to calculate the geometry of a complex containing cytosine and 14 water molecules. The results showed that the interaction of water molecules with cytosine resulted in significant changes to the molecular geometry in both the ground and excited states.[30,31] Considering the size of the solvation complex for cytosine, the opportunity for minor variations in the structure is great, potentially accounting for the large inhomogeneous line width.

Conclusions

The resonance Raman spectra and resulting analysis presented here provide insight into the photochemistry of cytosine. The most intense Raman bands are the 1283 and 1364 cm^{-1} bands. Although five of the observed modes are photochemically relevant, they all show relatively low intensity. Overall, at most, 31% of the reorganization energy upon UV excitation of cytosine is in photochemically relevant modes. This result suggests that cytosine is less primed for photochemistry than thymine but somewhat more primed then uracil. These results are significant for developing a molecular mechanism for UV-induced nucleic acid damage, with its important physiological consequences and implications for the origins of life.

Supporting Information Available: Figure containing the unmodified spectrum of cytosine between 2200 and 3000 cm^{-1} and the diode array adjusted and baseline corrected version of the same. This material is available free of charge via the Internet at http://pubs.acs.org.

References and Notes

(1) Lehninger, A. L. *Biochemistry*; Worth Publications: New York, 1975; Vol. 2, pp 309−333.

(2) Ruzsicska, B. P.; Lemaire, D. G. E. In *CRC Handbook of Organic Photochemistry and Photobiology*; Horspool, W. H., Song, P.-S., Eds.; CRC Press: New York, 1995; pp 1289−1317.

(3) (a) Kang, H.; Taek Lee, K.; Jung, B.; Jae Ko, Y.; Keun Kim, S. *J. Am. Chem. Soc.* **2002**, *124*, 12958−12959. (b) He, Y.; Wu, C.; Kong, W. *J. Phys. Chem. A* **2003**, *107*, 5145−5148.

(4) Pecourt, J.-M. L,; Peon, J.; Kohler, B. *J. Am. Chem. Soc.* **2000**, *122*, 9348−9349.

(5) Onidas, D.; Markovitsi, D.; Marguet, S.; Sharonov, A.; Gustavsson, T. *J. Phys. Chem. B* **2002**, *106*, 11367−11374.

(6) Peon, J.; Zewail, A. H. *Chem. Phys. Lett.* **2001**, *348*, 255−262.

(7) (a) Myers, A. B.; Mathies, R. A. In *Biological Applications of Raman Spectroscopy, Resonance Raman Spectra of Polyenes and Aromatics*; Spiro, T. G., Ed.; Wiley-Interscience: New York, 1987; Vol. 2, pp 1−58. (b) Myers, A. B. Excited Eletronic State Properties From Ground-state Resonance Raman Intensities. In *Laser Techniques in Chemistry*; Myers, A. B., Rizzo, T. R., Eds.; Wiley: New York, 1995; pp 325−384. (c) Kelley, A. M. *J. Phys. Chem. A* **1999**, *103*, 6891−6903.

(8) Fodor, S. P. A.; Rava, R. P.; Hays, T. R.; Spiro, T. G. *J. Am. Chem. Soc.* **1985**, *107*, 1520−1529.

(9) (a) Fodor, S. P. A.; Spiro, T. G.; *J. Am. Chem. Soc.* **1986**, *108*, 3198−3205. (b) Perno, J. R.; Grygon, C. A.; Spiro, T. G. *J. Phys. Chem.* **1989**, *93*, 5672−5678.

(10) Kubasek, W. L.; Hudson, B.; Peticolas, W. L. *Proc. Natl. Acad. Sci. U.S.A.* **1985**, *82*, 2369−2373.

(11) Blazej, D. C.; Peticolas, W. L. *J. Chem. Phys.* **1980**, *72*, 3134−3142.

(12) Yarasi, S.; Loppnow, G. R. *J. Am. Chem. Soc.*, submitted for publication, 2005.

(13) Webb, M. A.; Fraga, E.; Loppnow, G. R. *J. Phys. Chem.* **1996**, *100*, 3278−3287.

(14) Webb, M. A.; Kwong, C. M.; Loppnow, G. R. *J. Phys. Chem. B* **1997**, *101*, 5062−5069.

(15) Loppnow, G. R.; Fraga, E. *J. Am. Chem. Soc.* **1997**, *119*, 896−905.

(16) Mathies, R.; Oseroff, A. R.; Stryer, L. *Proc. Natl. Acad. Sci. U.S.A.* **1976**, *73*, 1−5.

(17) Fraga, E.; Loppnow, G. R. *J. Phys. Chem. B* **1998**, *102*, 7659−7665.

(18) Lee, S.-Y.; Heller, E. J. *J. Chem. Phys.* **1979**, *71*, 4777−4788.

(19) Mukamel, S. *Principles of nonlinear optical spectroscopy*; Oxford University Press: New York, 1995.

(20) Li, B.; Johnson, A. E.; Mukamel, S.; Myers, A. B. *J. Am. Chem. Soc.* **1994**, *116*, 11039−11047.
(21) Shoute, L. C. T.; Loppnow, G. R. *J. Chem. Phys.* **2002**, *117*, 842−850.
(22) Gaigeot, M. P.; Leulliot, N.; Ghomi, M.; Jobic, H.; Coulombeau, C.; Bouloussa, O. *Chem. Phys.* **2000**, *261*, 217−237.
(23) Santamaria, R.; Charro, E.; Zacarias, A.; Castro, M. *J. Comput. Chem.* **1998**, *20*, 511−530.
(24) Aamouche, A.; Ghomi, M.; Grajcar, L.; Baron, M. H.; Romain, F.; Baumruk, V.; Stepanek, J.; Coulombeau, C.; Jobic, H.; Berthier, G. *J. Phys. Chem. A* **1997**, *101*, 10063−10074.
(25) Durbeej, B.; Eriksson, L. A. *Photochem. Photobiol.* **2003**, *78*, 159.
(26) Callis P. R. *Annu. Rev. Phys. Chem.* **1983**, *34*, 329−357.
(27) Hug, W.; Tinoco, I. *J. Am. Chem. Soc.* **1973**, *95*, 2803−2813.
(28) Lagant, P.; Vertgoten, G.; Peticolas, W. L. *J. Raman Spectrosc.* **1999**, *30*, 1001−1007.
(29) Crespo-Hernández, C. E.; Cohen, B.; Hare, P. M.; Kohler, B. *Chem. Rev.* **2004**, *104*, 1977−2019.
(30) Shishkin, O. V.; Gorb, L.: Leszczynski, J. *J. Phys. Chem. B* **2000**, *104*, 5357−5361.
(31) Shukla, M. K.; Leszczynski, J. *J. Phys. Chem. A* **2002**, *106*, 11338−11346.